Properties of the 5^- state at 839 keV in ^{176}Lu and the *s*-process branching at $A = 176$

P. Mohr,[1,*] S. Bisterzo,[2] R. Gallino,[2] F. Käppeler,[3] U. Kneissl,[4] and N. Winckler[5]
[1]*Diakonie-Klinikum Schwäbisch Hall, D-74523 Schwäbisch Hall, Germany*
[2]*Dipartimento di Fisica Generale, Università di Torino, Via P. Giuria 1, I-10125 Torino, Italy*
[3]*Forschungszentrum Karlsruhe, Institut für Kernphysik, P. O. Box 3640, D-76021 Karlsruhe, Germany*
[4]*Institut für Strahlenphysik, Universität Stuttgart, Allmandring 3, D-70569 Stuttgart, Germany*
[5]*GSI, Planckstraße 1, D-64291 Darmstadt, Germany*
(Received 20 February 2009; published 10 April 2009)

The *s*-process branching at mass number $A = 176$ depends on the coupling between the high-K ground state and a low-lying low-K isomer in ^{176}Lu. This coupling is based on electromagnetic transitions via intermediate states at higher energies. The properties of the lowest experimentally confirmed intermediate state at 839 keV are reviewed, and the transition rate between low-K and high-K states under stellar conditions is calculated on the basis of new experimental data for the 839-keV state. Properties of further candidates for intermediate states are briefly analyzed. It is found that the coupling between the high-K ground state and the low-K isomer in ^{176}Lu is at least one order of magnitude stronger than previously assumed, leading to crucial consequences for the interpretation of the ^{176}Lu /^{176}Hf pair as an *s*-process thermometer.

DOI: 10.1103/PhysRevC.79.045804 PACS number(s): 26.20.Kn, 23.35.+g, 25.20.Dc, 27.70.+q

I. INTRODUCTION

Several studies have been devoted to the *s*-process branching at mass number $A = 176$ in the last years [1–4]. ^{176}Lu and ^{176}Hf are *s*-only nuclei and shielded from the *r*-process by stable ^{176}Yb. At first view, the abundance ratio between the unstable ^{176}Lu and the stable ^{176}Hf seems to be a perfect chronometer for the *s*-process because of the long β-decay half-life of ^{176}Lu of about 40 gigayears. However, this ground-state half-life of ^{176}Lu may be dramatically reduced under stellar conditions because of the coupling of the long-living $J^\pi = 7^-; K = 7$ ground state to a low-lying, short-living $1^-; 0$ isomer at $E_x = 123$ keV via so-called intermediate states (IS) at higher energies. The 1^- isomer in ^{176}Lu also β decays to ^{176}Hf with a short half-life of $t_{1/2} = 3.66$ h. The coupling depends sensitively on temperature that turns the chronometer into a thermometer for the helium shell flashes of AGB stars that are the commonly accepted stellar site of *s*-process nucleosynthesis [5]. The *s*-process branching at ^{176}Lu is schematically shown in Fig. 1.

Under *s*-process conditions most of ^{176}Lu (≈86%) is produced in the isomeric state in the ^{175}Lu$(n,\gamma)^{176}$Lu reaction [1]. At low temperatures the coupling between the low-K isomer and the high-K ground state is weak, and the isomer, i.e., almost all produced ^{176}Lu, β-decays to ^{176}Hf. At higher temperatures the increasing coupling depopulates the isomer and produces ^{176}Lu in its long-living ground state, thus increasing the ^{176}Lu abundance and the ^{176}Lu$(n,\gamma)^{177}$Lu branch. At very high temperatures the production of ^{176}Lu is reduced again because of the repopulation of the isomer when approaching thermal equilibrium.

Properties of candidates for IS have been carefully studied in a series of experiments. Photon scattering [6] and photoactivation of ^{176}Lu [7] have been measured using bremsstrahlung at the Stuttgart dynamitron, and earlier experiments with bremsstrahlung have been performed using medical and technical electron accelerators [8–11] that are known to provide high photon intensities [12]. Activation after Coulomb excitation was studied at the Tandem accelerator at IPN, Orsay [13], activation using positron annihilation was measured at the Kyoto research reactor [14], and photoactivation experiments with various radioactive sources were reported in Refs. [10,15–17]. High-resolution γ-spectroscopic studies were performed using the ^{175}Lu$(n,\gamma)^{176}$Lu reaction at the GAMS spectrometer at ILL, Grenoble [18–20], using HPGe detectors [19,21], and using the ^{176}Yb$(p,n)^{176}$Lu reaction at the Berkeley cyclotron [22]. The ^{177}Hf$(t,\alpha)^{176}$Lu reaction was studied at Los Alamos using a Q3D magnetic spectrograph [23], and the ^{175}Lu$(d,p)^{176}$Lu reaction was analyzed using the Q3D spectrograph at the Munich tandem accelerator [19]. Obviously, the *s*-process branching at $A = 176$ depends also on the neutron capture cross sections. These cross sections have been measured with high accuracy, see Refs. [1,4] and references therein, and will not be analyzed here again.

This article focuses on experimentally confirmed properties of ^{176}Lu and the well-established IS at an excitation energy of $E_x = 839$ keV with $J^\pi; K = 5^-; 4$. It will be shown that the coupling between the high-K $7^-; 7$ ground state and the low-K $1^-; 0$ isomer in ^{176}Lu via the IS at 839 keV is significantly stronger than adopted in the latest analysis [1]. A further enhancement of the coupling has been suggested from K mixing of two almost degenerate 7^- states at $E_x = 725$ keV [2].

This article is organized as follows: In Sec. II the formalism for the coupling of low-K and high-K states in a stellar photon bath will be reviewed. This article focuses on experimental results for the IS at 839 keV in Sec. III; here conclusions can be drawn that are firmly based on experimental data. Special attention will be given to a recent photoactivation experiment [7]. Contrary to these experimentally based results, the recent analysis of K mixing for the two 7^- states at 725 keV [2] has to

*WidmaierMohr@t-online.de

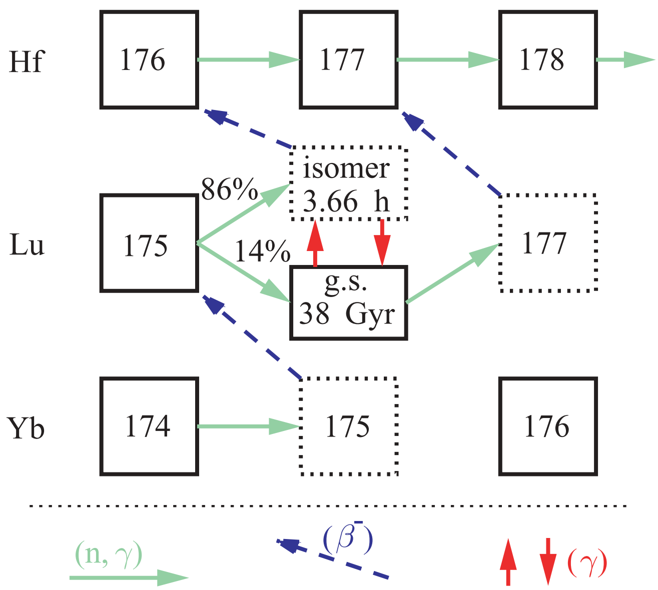

FIG. 1. (Color online) Schematic view of the s-process branching at $A = 176$. Stable (unstable) nuclei are shown with full (dotted) boxes. Note that the long-living ground state of ^{176}Lu is quasistable for the time scale of the s-process. Horizontal arrows indicate (n,γ) neutron capture reactions, the dashed arrows correspond to β^- decays, and the vertical arrows indicate the thermal coupling between the high-K ground state and the low-K isomer in ^{176}Lu. The ^{175}Lu$(n,\gamma)^{176}$Lu reaction mainly populates the isomer in ^{176}Lu (86%) and has only a weak 14% branch to the ground state [1].

rely on theoretical considerations. The interpretation of these experimental results for the 839-keV state and the translation from results under laboratory conditions to stellar conditions will be given in Sec. IV. Section V lists further candidates for low-lying IS. Astrophysical consequences will be discussed in Sec. VI. Finally, conclusions are given in Sec. VII.

II. STELLAR TRANSITION RATES BETWEEN LOW-K AND HIGH-K STATES

Direct transitions between low-K and high-K states are highly suppressed by K-selection rules. Typically, one finds suppression factors $F_W = \tau(\mathrm{exp})/\tau(\mathrm{W.u.})$ of the order of 100 per degree ν of K-suppression ($\nu = |\Delta K - \mathcal{L}|$) where $\tau(\mathrm{W.u.})$ is the Weisskopf estimate for the lifetime τ of an E$\mathcal{L}$ or M$\mathcal{L}$ electromagnetic transition [24].

It has been shown that thermal equilibrium is achieved within the low-K states and within the high-K states on a short time scale of by far less than 1 sec [2,25] that is much shorter than typical time scales in s-process nucleosynthesis [5,26], whereas transition rates between low-K states and high-K states are much slower and depend critically on temperature. Consequently, ^{176}Lu has to be considered as two different species, one with low K and one with high K, in nucleosynthesis calculations for the s process. The stellar transition rate λ^* for transitions between the high-K and the low-K species of ^{176}Lu is given by

$$\lambda^*(T) = \int c n_\gamma(E,T)\sigma(E)dE \approx c\sum_i n_\gamma(E_{\mathrm{IS,i}},T)I_\sigma(E_{\mathrm{IS,i}}) \quad (2.1)$$

with the thermal photon density

$$n_\gamma(E,T) = \left(\frac{1}{\pi}\right)^2\left(\frac{1}{\hbar c}\right)^3 \frac{E^2}{\exp(E/kT)-1} \quad (2.2)$$

and the energy-integrated cross section I_σ for an IS at excitation energy E_{IS}

$$I_\sigma = \int \sigma(E)dE = \frac{2J_{\mathrm{IS}}+1}{2J_0+1}\left(\frac{\pi\hbar c}{E_{\mathrm{IS}}}\right)^2 \times \frac{\Gamma_{\mathrm{IS}\to\mathrm{low-K}}\Gamma_{\mathrm{IS}\to\mathrm{high-K}}}{\Gamma} \quad (2.3)$$

$\Gamma_{\mathrm{IS}\to\mathrm{low-K}}$ and $\Gamma_{\mathrm{IS}\to\mathrm{high-K}}$ are the total decay widths from the IS to low-K and to high-K states (including all cascades), $\Gamma = \Gamma_{\mathrm{IS}\to\mathrm{low-K}} + \Gamma_{\mathrm{IS}\to\mathrm{high-K}}$ is the total decay width, J_{IS} and J_0 are the spins of the IS and the initial state, and the energy E_{IS} is given by the difference between the excitation energies of the IS and the initial state: $E_{\mathrm{IS}} = E_x(\mathrm{IS}) - E_0 = E_x(\mathrm{IS})$ for the transition rate λ^* from high-K to low-K states. The factor $\Gamma_{\mathrm{IS}\to\mathrm{low-K}} \times \Gamma_{\mathrm{IS}\to\mathrm{high-K}}/\Gamma$ in Eq. (2.3) may also be written as $b_{\mathrm{IS}\to\mathrm{low-K}} \times b_{\mathrm{IS}\to\mathrm{high-K}} \times \Gamma$ or $b_{\mathrm{IS}\to\mathrm{low-K}} \times b_{\mathrm{IS}\to\mathrm{high-K}} \times \hbar/\tau$ where $b_{\mathrm{IS}\to\mathrm{low-K}}$ and $b_{\mathrm{IS}\to\mathrm{high-K}}$ are the total decay branchings of the IS and $\tau = \hbar/\Gamma$ is its lifetime.

The total stellar transition rate in Eq. (2.1) is given by the sum over all IS; however, from the exponential dependence of the photon density in Eq. (2.2) it is obvious that only very few low-lying IS—and often only the lowest IS—dominate the stellar transition rate. It will be shown that the experimentally confirmed IS at 839 keV plays a key role that may be superseded if there is strong K mixing between the two 7^- states at 725 keV [2].

Finally, it has to be noted that the principle of detailed balance applies under stellar conditions to the transition rates from high-K to low-K states and its inverse from low-K to high-K states:

$$\frac{\lambda^*(\mathrm{low-}K \to \mathrm{IS} \to \mathrm{high-}K)}{\lambda^*(\mathrm{high-}K \to \mathrm{IS} \to \mathrm{low-}K)} \approx \frac{2J_{\mathrm{g.s.}}+1}{2J_{\mathrm{iso}}+1}\exp(E_{\mathrm{iso}}/kT), \quad (2.4)$$

with $J_{\mathrm{g.s.}} = 7^-$ (high-K), $J_{\mathrm{iso}} = 1^-$ (low-K), and $E_{\mathrm{iso}} = 123$ keV for ^{176}Lu. This ratio of reaction rates in Eq. (2.4) is independent of the properties of the IS. Under typical stellar conditions of the s-process the transition rate from the low-K isomer at 123 keV to the high-K ground state is much larger than its inverse rate that populates the isomer because $(2J_{\mathrm{g.s.}}+1)/(2J_{\mathrm{iso}}+1) = 5$ for ^{176}Lu and $\exp(E_{\mathrm{iso}}/kT) \gg 1$ at typical s-process temperatures; e.g., at $kT = 23$ keV—typical for the ^{22}Ne$(\alpha,n)^{25}$Mg neutron source during helium shell flashes—a ratio of about 1000 is found. For the lower temperature of about 8 keV—typical for the ^{13}C$(\alpha,n)^{16}$O neutron source—this ratio is even higher. However, at this low temperature the reaction rate is negligibly small, and the low-K states and the high-K states in ^{176}Lu are decoupled.

III. AVAILABLE EXPERIMENTAL DATA AND INTERPRETATION

As mentioned in the Introduction, various types of experimental data are available for the odd-odd nucleus ^{176}Lu. In particular, because of the stable neighboring ^{175}Lu it is possible to use the (n, γ) reaction for a detailed spectroscopic study that has been performed at the ILL using the ultra-high-resolution spectrometer GAMS [18–20]. In addition, neutron transfer in the ^{175}Lu$(d, p)^{176}$Lu reaction has been used in combination with a high-resolution Q3D magnetic spectrograph [19], and the ^{176}Yb$(p, n)^{176}$Lu reaction has been combined with high-resolution spectroscopy of HPGe detectors [22]. The obtained information is compiled in the ENSDF online database [27] that is based on Ref. [28]. Further information on IS can be deduced from a Coulomb excitation and activation experiment [13] that has detected the activity of the isomer in ^{176}Lu recoil nuclei after Coulomb excitation by a ^{32}S projectile and from various photoactivation experiments using bremsstrahlung and radioactive sources [8–11,15–17]. Finally, a photoactivation experiment has been performed [7] using the high photon flux of the bremsstrahlung setup of the dynamitron accelerator at Stuttgart [29]. Although a final analysis of these data is unfortunately not available, the data analysis in [7] is sufficient to derive the integrated cross section of the IS at 839 keV unambiguously in combination with the other available data [13,18–20].

The integrated cross section for the transition between low-K and high-K states depends on the lifetime τ and the branchings b of the IS, see Eq. (2.3) in Sec. II and the following text. Thus, two different approaches have been followed to determine the integrated cross section I_σ of the IS at 839 keV. For illustration, a partial level scheme of ^{176}Lu is shown in Fig. 2.

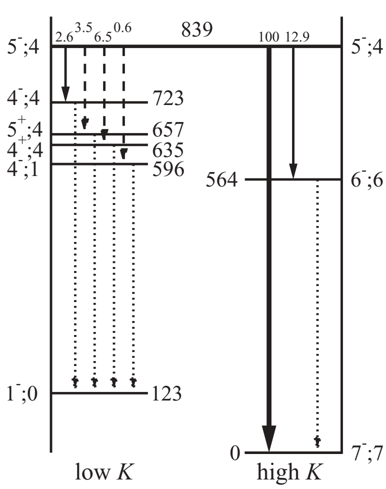

FIG. 2. Partial level scheme of ^{176}Lu with low-K states on the left and high-K states on the right. The IS at 839 keV decays to low-K and to high-K states. Observed γ-ray lines are indicated by solid arrows. Dashed lines show tentative decays of the IS at 839 keV. Relative γ-ray branches $b^\gamma_{\rm rel}$ normalized to the dominating ground-state branching $b^\gamma_{\rm rel}(839 \to 0) = 100$ are given for the IS at 839 keV. The dotted lines represent cascade transitions to the high-K $7^-;7$ ground state and to the $1^-;0$ isomer at 123 keV that is the lowest low-K state.

In a first approach, see Sec. III B, high- and ultra-high γ-spectroscopic studies have been performed to measure γ-ray branching ratios. This first approach clearly identifies IS from the measured branching ratios b to low-K and high-K states; however, an additional measurement of the lifetime τ of the IS has to be performed that is difficult for the relevant lifetimes of the order of several picoseconds. Lifetime measurements are further complicated by feeding in the complex decay scheme of the heavy odd-odd nucleus ^{176}Lu [21]. It turns out that this first approach is ideal for the identification of IS but of limited applicability for the determination of integrated cross sections.

In a second approach, see Sec. III C, photoactivation experiments have been performed. The photoactivation yield is directly proportional to the integrated cross section $I_\sigma^{\rm lab}$ of the contributing IS, i.e., this measurement provides integrated cross sections I_σ but does not provide the ingredients for I_σ that are the branching b and the lifetime τ. Because of the typically broad spectral shape of the incoming photons it is difficult to assign the photoactivation yield directly to a particular IS. This argument holds for experiments with radioactive sources, bremsstrahlung, and virtual photons in Coulomb excitation.

It will be shown in Sec. III D that the combination of the high-resolution γ-spectroscopic studies (first approach) and photoactivation results (second approach) allows the first unique determination of the integrated cross section I_σ of the IS at 839 keV. The combined analysis leads to a reduction of the uncertainty of I_σ from about two orders of magnitude to about a factor of two.

A. Photoactivation at the Stuttgart dynamitron

The recent photoactivation experiment performed at the Stuttgart dynamitron accelerator plays an essential role in this analysis. We briefly review the results given only in conference proceedings until now [7]. Details of the experiment will be published elsewhere [30].

The high-current dynamitron accelerator at the IfS Stuttgart provides high bremsstrahlung intensities up to energies of 4 MeV and allows for very sensitive photoactivation studies [31,32]. Details of the accelerator and the experimental setup are given in [29]. Lutetium samples with natural isotopic composition and masses of about 9 mg of ^{176}Lu (total mass about 350 mg) were irradiated with bremsstrahlung at end-point energies from about 800 keV to 3 MeV. Small steps in the end-point energy were used to assign the photoactivation yield to particular IS that is otherwise a serious limitation of photoactivation experiments (see above, "second approach"). The isomer population via IS was detected by decay γ-spectroscopy of the 88-keV line from the ^{176}Lu$^{\rm m} \to {}^{176}$Hf decay at higher end-point energies. However, a practically constant background in this γ-ray line is found from the decay of the long-living ^{176}Lu ground state. To improve the sensitivity, β spectroscopy has been used to detect electrons with energies above the end point of the ^{176}Lu ground-state decay. From both β- and γ-spectroscopy data the half-life of the isomer could be determined with $t_{1/2} = 3.63 \pm 0.02$ h (γ-spectroscopy) and 3.640 ± 0.004 h (β-spectroscopy); these results are in good agreement with the adopted half-life of 3.664 ± 0.019 h [27]. The measured events in the γ and β

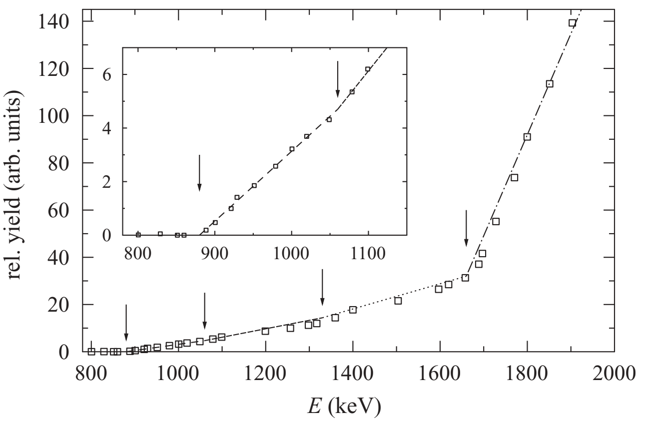

FIG. 3. Experimental yield of the photoactivation of ^{176}Lu as a function of the end-point energy E. Kinks in the yield curve correspond to IS and are marked by vertical arrows. Between two IS the yield increases almost linearly, and the slope of the lines is proportional to the integrated cross section I_σ. The inset shows the low-energy region with the lowest IS at 880 ± 30 keV and the second IS at 1060 ± 30 keV. The lines between IS can be used to estimate the relative values of the integrated cross sections I_σ.

detectors have been properly corrected taking into account the decay of ^{176}Lu^m during the irradiation, the short waiting time between irradiation and counting, and during the counting time. The derived experimental yield is shown in Fig. 3 in arbitrary units.

The experimental photoactivation yield from a particular IS is proportional to the integrated cross section I_σ and increases almost linearly with the end-point energy of the bremsstrahlung. As long as the end-point energy remains below the lowest IS, the experimental yield obviously vanishes. When the first IS is reached, the experimental yield starts to increase roughly linearly. Whenever the end-point energy exceeds a further IS, the slope of the yield curve increases because of the additional contribution of this IS. A schematic view of these properties of the yield curve is shown in Fig. 1 of Ref. [29].

The experimental yield is shown in Fig. 3 for end-point energies between 800 keV and 2 MeV. A clear evidence for IS is found from the kinks of the yield curve that are located at 880, 1060, 1330, and 1660 keV. The uncertainty of the energies of the IS is about 30 keV that is composed mainly of the uncertainty of the experimental end-point energies and of the finite energy steps in the yield curve in Fig. 3. This limited energy resolution complicates the assignment of the kinks in the yield curve to individual IS in ^{176}Lu. The energy difference between the lowest IS and the second IS is $\Delta E = 180 \pm 15$ keV. The smaller uncertainty of about 15 keV for the energy difference can be obtained because the error in the end-point assignment is approximately the same for all measurements between 800 and 1200 keV.

From the changes of the slope in the yield curve between IS (see Fig. 3) a rough estimate for the relative strength of the integrated cross sections I_σ for the lowest IS can be derived. The cross sections behave like 1:0.4:0.7:14.3 for the first four IS in ^{176}Lu at 880, 1060, 1330, and 1660 keV.

B. High-resolution γ-spectroscopic data (“first approach”)

The dominating decay of the IS is the direct $E2$ transition from the 5^- IS at 839 keV to the 7^- ground state. Firmly assigned is the intraband transition from the 5^- IS to its 4^- band head of the $K = 4$ band at 723 keV. This 4^- state decays via a γ-ray cascade down to the $1^-;0$ isomer at 123 keV (see Fig. 2). Thus, the properties of the 5^- state at 839 keV as IS are experimentally clearly confirmed. Further, there are several tentative assignments for transitions from the 5^- IS at 839 keV to low-K states that finally end at the 1^- isomer at 123 keV. Depending on these tentative assignments, the γ-ray branching to the low-K isomer is [19]

$$0.021 \leqslant b^{\gamma}_{\mathrm{IS}\rightarrow\mathrm{low-K}} \leqslant 0.105. \tag{3.1}$$

Using these γ-ray branchings and theoretically estimated conversion coefficients [33], this leads to

$$0.065 \leqslant b^{\gamma+\mathrm{CE}}_{\mathrm{IS}\rightarrow\mathrm{low-K}} \leqslant 0.149 \tag{3.2}$$

for the branching $b^{\gamma+\mathrm{CE}}$ including conversion electrons in neutral ^{176}Lu. The branching under stellar conditions b^* will be in between the lower limit of the γ-ray branching b^γ and the upper limit of the branching including conversion electrons $b^{\gamma+\mathrm{CE}}$:

$$b^{\gamma}_{\mathrm{min}} \leqslant b^* \leqslant b^{\gamma+\mathrm{CE}}_{\mathrm{max}} \tag{3.3}$$

$$0.021 \leqslant b^* \leqslant 0.149. \tag{3.4}$$

The precise value of b^* depends on the degree of ionization at a given stellar temperature T. It can be estimated using the formalism in Ref. [34] that leads to about $n^*_K \approx 0.4$ electrons in the K-shell at $kT = 23$ keV instead of $n_{\mathrm{K}} = 2$ for neutral atoms.

It is obvious that the low-energy bremsstrahlung in the photoactivation experiment [7] is not able to produce highly ionized ^{176}Lu. The same argument holds for all photoactivation experiments with radioactive sources [10,15–17] and for the activation experiment after Coulomb excitation where the recoiling ^{176}Lu nucleus has relatively low energies. Thus, activation experiments in the laboratory determine $b^{\gamma+\mathrm{CE}}$ instead of b^γ or b^* (see also Secs. III C and IV). Note that the conversion coefficient for low-energy transitions is mainly defined by the strongest bound K-shell electrons.

It has been attempted to measure the lifetime τ of the IS at 839 keV in Refs. [18–20] that is mainly defined by the strongest transition from the IS to the ground state. An upper limit could be obtained from the measured time distributions using the generalized centroid-shift method [19], and a lower limit was obtained from the γ-ray induced Doppler broadening (GRID) technique [18]. The combined result is

$$10\,\mathrm{ps} \leqslant \tau \leqslant 433\,\mathrm{ps}. \tag{3.5}$$

Note that the half-life $t_{1/2} \leqslant 300$ ps has been determined in the original work [19] that is later cited—probably in error—as lifetime $\tau \leqslant 300$ ps [1,18,20]. A recent photon-scattering experiment [6] did not see the IS at 839 keV; from the experimental limits $\tau \geqslant 1.5$ ps could be derived that does not further restrict the allowed range for the lifetime τ in Eq. (3.5).

The combination of the branching ratios b^γ, $b^{\gamma+\mathrm{CE}}$, and b^* in Eqs. (3.1), (3.2), and (3.4), and the lifetime τ in Eq. (3.5) leads to the following integrated cross sections

$$12.5 \text{ meV fm}^2 \leqslant I_\sigma^{\text{f.i.}} \leqslant 2479 \text{ meV fm}^2 \quad (3.6)$$

$$37.1 \text{ meV fm}^2 \leqslant I_\sigma^{\text{lab}} \leqslant 3344 \text{ meV fm}^2 \quad (3.7)$$

with the value I_σ^{lab} calculated for neutral ^{176}Lu using the branching $b^{\gamma+\text{CE}}$ including conversion electrons, and the value $I_\sigma^{\text{f.i.}}$ for fully ionized ^{176}Lu using the γ-ray branching b^γ. Again, the stellar value I_σ^* will be in between the laboratory result and the result for fully ionized ^{176}Lu.

In addition to the IS at 839 keV, further IS at higher energies have been detected in the γ-spectroscopic experiments [19,22]. Decay branches to the low-K and to the high-K part of the ^{176}Lu level scheme have been reported for the $5^-;4$ state at 922 keV, the $6^-;4$ state at 963 keV, the 5^- state at 1032 keV, and the $5^-;3$ state at 1069 keV. Only for the 922 keV IS is an upper limit of $\tau < 290$ ps is available [19] that translates together with the measured branching ratios to a lower limit of the integrated cross section $I_\sigma \gtrsim 100$ meV fm^2. No lifetime information is available for the IS at 963 keV, 1032 keV, and 1069 keV; it is impossible to derive the integrated cross sections I_σ for these IS from the γ-spectroscopic data. Furthermore, the IS at 963 and 1069 keV cannot be seen in photoactivation because of the missing ground-state branch [27].

Summarizing the high-resolution γ-spectroscopic experiments, a clear assignment of IS is possible but the integrated cross section I_σ of the IS at 839 keV remains uncertain by about two orders of magnitude, and I_σ for other IS cannot be determined.

C. Photoactivation experiments (“second approach”)

Because of the dominating ground-state decay of the IS at 839 keV it is possible to measure the integrated cross section I_σ by photoactivation experiments [7,13] (see also Sec. IV). Other branches from the IS at 839 keV to high-K states in ^{176}Lu contribute only by about 10 %; this marginal correction to the integrated cross section I_σ^* is neglected in the following.

Photoactivation experiments have been performed with bremsstrahlung, radioactive sources, and virtual photons in Coulomb excitation. There is general agreement between the various types of activation studies that the experimental yield rises steeply with energy. This indicates that there are IS with large integrated cross sections at higher energies. However, these IS at higher energies are not relevant under s-process conditions. Consequently, it is not possible to derive properties of low-lying IS from bremsstrahlung photoactivation experiments with end-point energies of several MeV [8,9,11]. There is also general agreement that the lowest IS is located at energies above 650 keV because photoactivation of ^{176}Lu could not be observed after irradiation with ^{137}Cs sources ($E_\gamma = 662$ keV) [10,16,17] and in an experiment with bremsstrahlung with an end-point energy of 600 keV [10]. A clear photoactivation signal has been observed using higher-energy γ-ray sources ^{60}Co ($E_\gamma = 1332$ keV and 1173 keV) [10,15–17] and ^{24}Na ($E_\gamma = 2754$ keV and 1369 keV) [10]. All these findings are nicely confirmed by the measured yield curve in Fig. 3.

In general, the yield in photoactivation experiments with broad incoming photon spectra determines a weighted sum of integrated cross sections I_σ for all IS within the photon spectrum. The contribution of a particular IS is weighted by the relative spectral intensity of the incoming photons. The assignment of an experimental yield to a particular IS is thus complicated. This holds for all photoactivation experiments under discussion. Bremsstrahlung spectra are very broad from $E_\gamma \approx 0$ up to the end point of the incoming electron beam. The primary spectra from radioactive sources are line spectra. However, these line spectra are broadened by Compton scattering within the heavy shielding of strong sources. Virtual photon spectra in Coulomb excitation are also broad and can be modified by the choice of projectile, target, and incoming projectile energy.

Effective cross sections of 45 nb [10,15] and 38 nb [16] have been reported for photoactivation using ^{60}Co sources. The cross section for ^{24}Na irradiation is about a factor of 500 higher [10]. The ^{60}Co result of Ref. [15] has been translated to an integrated cross section of $I_\sigma \approx 6$–7 eV fm^2 under the assumption of an IS located at 1 MeV [10,17]. The photoactivation experiment after Coulomb excitation [13] reports $b^{\gamma+\text{CE}} \times (1 - b^{\gamma+\text{CE}})/\tau = 12^{+10}_{-6} \times 10^9$ s^{-1} that translates to an integrated cross section $I_\sigma^{\text{lab}} = 3164^{+2637}_{-1582}$ meV fm^2 for the strength of IS below 1 MeV excitation energy in ^{176}Lu with an uncertainty of a factor of two.

D. Combination of the two approaches

Although the photoactivation experiment using bremsstrahlung [7] does not provide integrated cross sections yet, this experiment does provide rough information on the excitation energies of the lowest IS from the kinks in the measured yield curve (see Fig. 3). The lowest IS is located at 880 ± 30 keV, and the next IS is found at 1060 ± 30 keV. The energy difference between the first and second IS is much better defined by $\Delta E = 180$ keV with an estimated uncertainty of about 15 keV. The comparison with the known IS from the γ-spectroscopic studies [19,22] leads to the clear conclusion that only the IS at 839 and 1032 keV with $\Delta E = 193$ keV have been seen in the photoactivation experiment [7], whereas the state at 922 keV does not show up in the photoactivation yield curve. From the yield curve in Fig. 3 an upper limit for the integrated cross section of the IS at 922 keV can be estimated that is about a factor of five lower than the integrated cross section for the 839-keV state. As will be shown below, this finding is in agreement with the lower limit for $I_\sigma \gtrsim 100$ meV fm^2 for this IS from the γ-spectroscopic data.

The kinks in the yield curve of Fig. 3 at higher energies (1330 and 1660 keV) cannot be assigned to IS from γ spectroscopy because the highest energies in the γ-spectroscopic studies were 1130 keV [19] and 902 keV [22]. A very tentative assignment can be suggested for the kink at 1330 keV. It may correspond (i) to the 1332-keV level seen in photon scattering and thus coupled to the ground state [6] or (ii) to a level at 1301 keV seen in the ^{176}Yb$(p,n)^{176}$Lu reaction [22] that is coupled to the isomer. A few levels around the IS at 1660 keV are reported in Ref. [27] at 1617, 1655, 1679, 1689, and 1693 keV however, for two of these levels not even a spin-parity assignment has been adopted in Ref. [27].

The photoactivation experiment after Coulomb excitation [13] is not able to resolve individual IS. The given result in Ref. [13] of $b^{\gamma+\mathrm{CE}} \times (1 - b^{\gamma+\mathrm{CE}})/\tau = 12^{+10}_{-6} \times 10^9\ \mathrm{s}^{-1}$ translates to an integrated cross section $I_\sigma^{\mathrm{lab}} = 3164^{+2637}_{-1582}$ meV fm^2 for the strength of IS below 1-MeV excitation energy in ^{176}Lu with an uncertainty of a factor of two. Because the γ-spectroscopic experiments [19] find only two IS below 1-MeV excitation energy, namely at 839 and 922 keV, the measured activation cross section must be the sum of the cross sections of both states. The next IS is reached at a significantly higher energy of 1032 keV that is more than 100 keV above the 922-keV state and 193 keV above the 839-keV state.

Because the 922-keV state does not contribute to the photoactivation yield in the bremsstahlung experiment, this state also cannot contribute to the Coulomb activation yield. Thus, the integrated cross section $I_\sigma^{\mathrm{lab}} = 3164$ meV fm^2 from the Coulomb excitation experiment [13] is dominated by the contribution of the IS at 839 keV; more than 80% of the strength in Ref. [13] can be assigned to the 839-keV IS. This result is at the upper end of the allowed range of I_σ^{lab} in Eq. (3.7) that has been determined from γ-spectroscopy experiments [18,19]. Combining the limits of the γ-spectroscopy experiments and the integrated cross section from the Coulomb excitation and photoactivation experiments leads to the conclusion that the branching $b^{\gamma+\mathrm{CE}}$ must be at the upper end of the allowed range in Eq. (3.2), and the lifetime τ of the IS at 839 keV must be close to the lower limit of Refs. [18,19]. A consistent set of parameters for the IS at 839 keV is $b^{\gamma+\mathrm{CE}} \approx 0.1$ and $\tau \approx 12$ ps leading to an integrated cross section $I_\sigma^{\mathrm{lab}} \approx 2000$ meV fm^2 with an upper limit of about 3500 meV fm^2 from the branching and the lifetime from γ-spectroscopic studies [18–20,22] and a lower limit of about 1250 meV fm^2 from the activation experiments [7,13]. In total, an uncertainty of a factor of two for the integrated cross section I_σ^{lab} seems to be a careful realistic estimate.

This result is also in reasonable agreement with the photoactivation using ^{60}Co sources with a maximum energy of $E = 1332$ keV. The integrated cross sections of the 839-, (922-), 1032-, and 1330-keV IS scale like 1:($\leqslant 0.2$):0.4:0.7 (see Fig. 3 and Sec. III A), i.e., about one half of the measured cross section of 6–7 eV fm^2 must be assigned to the lowest IS at 839 keV. However, this assignment to the lowest IS has a rather large uncertainty because the IS at 1330 ± 30 keV is located very close to the ^{60}Co energy of 1332 keV. Additionally, a tentative state in ^{176}Lu has been seen in photon scattering [6] at 1332 keV. If there is accidental overlap between the primary ^{60}Co energy and the excitation energy of an IS in ^{176}Lu, then the yield in the ^{60}Co photoactivation experiments [10,15–17] may be strongly affected by this IS at 1330 keV.

At first view, from the allowed ranges of I_σ^{lab} from γ spectroscopy in Eq. (3.7) and the result $I_\sigma^{\mathrm{lab}} = 3164^{+2637}_{-1582}$ meV fm^2 from the Coulomb activation experiment [13] a slightly higher result of $I_\sigma^{\mathrm{lab}} \approx 3000$ meV fm^2 should be derived. However, the limit from γ spectroscopy is a combined limit from two independent measurements of the branching ratio and the lifetime. A result of $I_\sigma^{\mathrm{lab}} \approx 3000$ meV fm^2 would require that both quantities are very close to their experimental limits that is statistically not very likely. Taking into account the relatively large uncertainties of the Coulomb activation experiment, $I_\sigma^{\mathrm{lab}} \approx 2000$ meV fm^2 seems to be a more realistic estimate for the integrated cross section of the IS at 839 keV in ^{176}Lu. A similar result is obtained from the average of the combined lower and upper limits from γ-spectroscopy and Coulomb activation.

E. Some further considerations

From the above parameters of the 839-keV state a surprisingly strong transition is found from the $7^-; 7$ ground state to the $5^-; 4$ IS at 839 keV. The lifetime $\tau = 12$ ps corresponds to roughly 3 W.u. that is much larger than the expected strength of about 0.01 W.u. for a K-forbidden $E2$ transition with $\Delta K = 3$ and thus $\nu = 1$. Contrary to the 839-keV state, the much smaller ground-state transition strength for the 922-keV state with the same quantum numbers $5^-; 4$ seems to be regular.

The strength of the transition from the $7^-; 7$ ground state to the $5^-; 4$ IS at 839 keV has also been estimated theoretically from the measured intraband branching of the 839-keV state to its $4^-; 4$ band head at 723 keV and the calculated strength of this intraband transition [18]. It is concluded in Ref. [18] that "the estimates ... point at a lifetime of the 838.6 keV level which is certainly below 50 ps, probably close to the lower experimental limit of 10 ps," although no explanation was found for the unusually large strength of this transition in Ref. [18].

There is one further experimental hint that the 839-keV state couples stronger to the high-K ground state of ^{176}Lu than the 922-keV state. Thermal s-wave neutron capture on ^{175}Lu with $J^\pi = 7/2^+$ populates mainly states with $J^\pi = 3^+, 4^+$ in ^{176}Lu. These states that obviously cannot be members of high-K bands will preferentially decay to low-K states. It is found that the number of observed γ rays per neutron capture for the $839 \to 0$ transition is about a factor of 5.5 larger than for the $922 \to 0$ transition [19]. This experimental finding further strengthens the result that there is an unusually strong coupling of the 839-keV IS to the high-K ground state.

IV. LABORATORY AND STELLAR REACTION RATES

In general, dramatic changes may be found for photon-induced reaction rates under laboratory and under stellar conditions. Whereas under laboratory conditions the target nucleus is in its ground state (except the case of ^{180}Ta that is found in nature in its long-living isomeric state), under stellar conditions excited states are populated in thermal equilibrium according to the Boltzmann statistics. Consequently, the transition rate under laboratory conditions depends on the direct decay width $\Gamma_{\mathrm{IS}\to\mathrm{g.s.}}$ to the ground state, whereas under stellar conditions the rate depends on the total γ-decay width to all states that finally cascade down to the ground state; in the case of ^{176}Lu this width is given by $\Gamma_{\mathrm{IS}\to\mathrm{high}-K}$ to all high-K states. A detailed discussion of the importance of thermally excited states under stellar conditions is given in Refs. [35,36].

For the case of ^{176}Lu the influence of thermally excited states is unexpectedly low. The dominating IS at 839 keV decays preferentially to the ground state, and the transition rate under stellar conditions is only moderately enhanced because $\Gamma_{\mathrm{IS}\to\mathrm{g.s.}} \approx \Gamma_{\mathrm{IS}\to\mathrm{high-K}}$. Compared to other uncertainties, this moderate enhancement of the order of 10–20% can be neglected in this work.

However, there is another effect that has to be analyzed. The only firmly assigned transition from the 5^- IS at 839 keV to low-K states in ^{176}Lu is the intraband transition to the band head of the $K = 4$ band at 723 keV with a relatively small transition energy of 116 keV. This $M1$ or $E2$ transition is enhanced by internal conversion for neutral ^{176}Lu atoms with conversion coefficients $\alpha_{M1} = 2.42$ and $\alpha_{E2} = 1.93$ [33]. This transition has been tentatively assigned to ($M1$) in Ref. [19]. Because of the relatively small difference of the $M1$ and $E2$ conversion coefficients, only the $M1$ assignment is used in the following discussion.

In laboratory experiments the charge state of ^{176}Lu depends on the experimental conditions. Under stellar conditions ^{176}Lu is highly ionized depending mainly on the temperature T and weakly on the electron density n_e [34]. The $M1$ conversion coefficient is mainly defined by the K-shell contribution. In all experiments under study in this article [7,13,18–22] ^{176}Lu will not be fully ionized. This is obvious for the neutron capture experiments with thermal neutrons [18–20] and the photoactivation with low-energy bremsstrahlung [7]. But also for the ^{175}Lu(d, p)^{176}Lu [19], ^{176}Yb(p, n)^{176}Lu [22], and Coulomb excitation and activation experiments [13] the energies are not sufficient to produce fully ionized ^{176}Lu. Thus, the derived transition strengths and integrated cross sections I_σ^{lab}, see Eq. (3.7), from the activation experiments can be compared to the γ-spectroscopic results including conversion electrons, and a combined result $I_\sigma^{\mathrm{lab}} \approx 2000$ meV fm^2 has already been given in Sec. III B.

At typical stellar s-process conditions [thermal energy $kT = 23$ keV, electron density $n_e = (3 - 5) \times 10^{26}$ cm^{-3}] the K shell of ^{176}Lu is partially ionized leading to $n_K^* \approx 0.4$ instead of $n_K = 2$ for neutral atoms. Thus, the decay width for the high-K $\to$ low-K transition with $E = 116$ keV has to be reduced by the factor $(1 + \alpha_{\mathrm{eff}})/(1 + \alpha_{\mathrm{lab}}) \approx 0.43$ with $\alpha_{\mathrm{eff}} \approx \alpha_{\mathrm{lab}} \times n_K^*/2$ leading to an integrated cross section of $I_\sigma^* \approx 850$ meV fm^2 under stellar s-process conditions.

The reduction factor $(1 + \alpha_{\mathrm{eff}})/(1 + \alpha_{\mathrm{lab}}) \approx 0.43$ is valid only for the low-energy transition with $E = 116$ keV. There are further tentative assignments for transitions from the 839-keV IS to low-K states with higher transition energies of $E = 181$, 203, and 243 keV. The conversion coefficients for these transitions are significantly smaller with $\alpha_{\mathrm{lab}} < 1$ compared to the 116-keV transition with $\alpha_{\mathrm{lab}} = 2.42$. The reduction factor $(1 + \alpha_{\mathrm{eff}})/(1 + \alpha_{\mathrm{lab}})$ remains close to unity for these tentatively assigned transitions. As the found branching $b^{\gamma+\mathrm{CE}}$ to low-K states (see at the end of Sec. III B) is about 0.1, it is very likely that not only the firmly assigned transition but also some tentatively assigned transitions contribute to the total transition strength from the IS at 839 keV to low-K states. Consequently, the reduction factor from I_σ^{lab} for neutral ^{176}Lu to the stellar I_σ^* for partially ionized ^{176}Lu is between the minimum value of $\approx$0.43 for the 116-keV transition and the maximum value of unity.

Combining all the above information and its uncertainties, the final result for the integrated cross section from high-K to low-K states via the IS at 839 keV under stellar s-process conditions is

$$600 \text{ meV fm}^2 \leqslant I_\sigma^* \leqslant 2500 \text{ meV fm}^2, \qquad (4.1)$$

which is entirely based on experimental results and reliably calculated internal conversion coefficients and stellar ionization. In short, this result can also be given as $I_\sigma^* \approx 1200$ meV fm^2 with an uncertainty of a factor of about two. In Sec. V the resulting reaction rate via the 839-keV state will be compared to other candidates for IS.

V. FURTHER CANDIDATES FOR LOW-LYING INTERMEDIATE STATES

The reaction rates from the high-K ground state to the low-K isomer in ^{176}Lu are shown for various IS in Fig. 4. Because of the dominance of the IS at 839-keV state, further candidates for IS are only briefly discussed.

In general, properties of astrophysically relevant IS should be an intermediate K quantum number and a low excitation energy. The transition rate λ^* depends linearly on the integrated cross section I_σ^* and exponentially on the excitation energy E_{IS}. The discussion in this Sec. V has to rely on theoretical considerations because the relevant properties of most

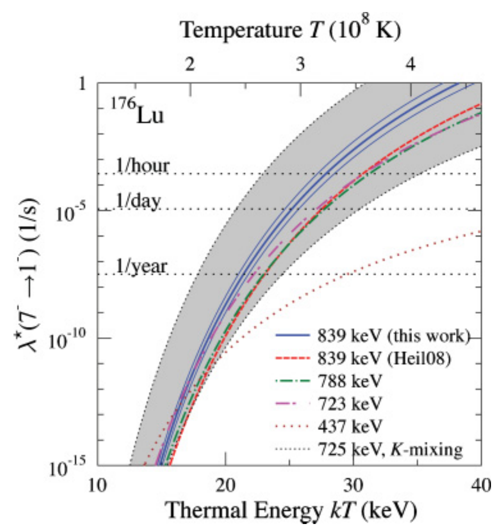

FIG. 4. (Color online) Reaction rates λ^* under stellar conditions for the transition from the high-K ground state to the low-K isomer in ^{176}Lu from Eqs. (2.1) and (2.3). The dominating IS is located at 839 keV; this rate is shown as thick full line (blue) with its uncertainties (thin full lines). A huge uncertainty remains for the theoretically estimated contribution from K mixing of two almost degenerate 7^- states at 725 keV [2] (thin dotted lines and gray shaded uncertainty). Contributions of other candidates for IS are small at $kT \approx 23$ keV, i.e., at s-process temperatures. A recent astrophysically derived transition rate [1] is also shown (red dashed line) that is at least one order of magnitude smaller than the result of this work. Further discussion see text.

candidates for IS have not been determined experimentally: whereas γ-spectroscopic data [19,20] clearly identify candidates for IS by their decay branches to low-K and high-K states, the integrated cross section I_σ cannot be derived from experiment because of missing lifetime data. Because of the relatively huge uncertainties of the lifetimes from theoretical Weisskopf estimates, a further correction of the data because of weakened internal conversion under stellar conditions—typically of the order of a factor of two or less—is neglected here.

Good candidates for further IS are the band heads of the $K = 4$ bands at 723 and 788 keV. Both 4^- states decay preferentially to a 3^- state at 658 keV that finally cascades down to the 1^- isomer. Both 4^- states may branch to a $6^-; 6$ high-K state at 564 keV although this branching has not been observed experimentally. Assuming one Weisskopf unit for this allowed $\Delta K = 2\,E2$ transition, the integrated cross sections are $I_\sigma^* \approx 10$ meV fm^2 for the 788-keV state and $I_\sigma^* \approx 2$ meV fm^2 for the 723-keV state. The reaction rate of both 4^- states (dash-dotted lines in Fig. 4) is significantly lower at $kT = 23$ keV than the 839-keV rate that is shown as thick solid line with its uncertainties (thin solid lines). The strength of the K-allowed direct $M3$ or $E4$ transition from the 4^- states to the 7^- ground state is negligible compared to the above mentioned $E2$ strength.

The $5^-; 0$ low-K state at 437-keV decays by γ cascades to the 1^- isomer. The strength of the unobserved K-forbidden $E2$ transition to the high-K ground state can be estimated from the K-forbiddenness $\nu = 5$ leading to 10^{-10} W.u. for this transition and $I_\sigma^* = 1.1 \times 10^{-7}$ meV fm^2. Although the 437-keV state has a much lower excitation energy than the other IS, this strength is by far not sufficient for a noticable contribution to the transition rate λ^* (dotted line in Fig. 4).

K mixing of two almost degenerate 7^- states at 725 keV has been studied in detail in Ref. [2]. Based on the results in Table I of Ref. [2] the transition rate can be calculated; the thin dotted lines and the gray shaded area show the allowed range of Ref. [2]. At the relevant energy of $kT = 23$ keV the contribution of K mixing may be larger or much lower than the experimentally confirmed transition rate of the 839-keV state. It is obvious that the decay branches of these two 7^- states have to be studied experimentally before a clear conclusion on the relevance of K mixing can be drawn. From the experimental limits of unobserved γ transitions from the two 7^- states in Ref. [19] a rough estimate for an upper limit of the integrated cross section and transition rate may be estimated that is about one order of magnitude lower than the result for full K mixing shown in Fig. 4 [2,37].

Additionally, Fig. 4 shows the result of an astrophysical determination (see Sec. VI) of the transition rate of the IS at 839 keV with an integrated cross section $I_\sigma^* = 71$ meV fm^2 [1] (dashed line) that is at least one order of magnitude smaller than the experimental result derived in Secs. III and IV.

Higher-lying IS have a negligible contribution to the total reaction rate. From the combination of the γ-spectroscopic data [19] and the photoactivation yield in Fig. 3 the integrated cross section of the IS at 922 keV is 100 meV fm$^2 \lesssim I_\sigma \lesssim$ 500 meV fm^2. Compared to the IS at 839 keV, the contribution of the IS at 922 keV is suppressed by its smaller I_σ and the higher excitation energy. A similar consideration for the IS at 1032 keV leads to an integrated cross section of about $I_\sigma \approx$ 1.4 eV fm^2 with an uncertainty of at least a factor of two. Together with the measured branchings of the IS at 1032 keV a lifetime of $\tau \approx 25$ ps can be derived for this state.

VI. ASTROPHYSICAL CONSEQUENCES

^{176}Lu and ^{176}Hf are produced in the so-called main component of the s-process that is assigned to thermally pulsing low-mass AGB stars [5,26,38]. The s-process branching at $A = 176$ is of special interest because this branching depends very sensitively on the temperature during s-process nucleosynthesis, whereas most other s-process branchings depend on the neutron density.

Two neutron sources operate in thermally pulsing AGB stars. The ^{13}C$(\alpha, n)^{16}$O reaction operates during the interpulse phase at relatively low temperatures of about $kT \approx 8$ keV for about 10^4 years; it releases about 90% of the total neutron exposure. The ^{22}Ne$(\alpha, n)^{25}$Mg reaction operates during the convective helium shell flashes at temperatures of about $kT \approx$ 23 keV that last for about 6 years; the temperature increases with the number of the thermal pulse and reaches a maximum of about $kT \approx 27$ keV [39].

The lower temperature of about 8 keV in the interpulse phase is not sufficient for a thermal coupling between the high-K ground state and the low-K isomer in ^{176}Lu. The reaction rate λ^* drops below about 10^{-15}/s $\approx 3 \times 10^{-8}$/y already above 12 keV (see Fig. 4) and is thus neglibible at 8 keV. The high-K ground state and the low-K isomer have to be treated as two fully separated species in this interpulse phase. However, at the higher temperature during the helium shell flashes the thermal coupling becomes effective.

Because of the sensitivity of the thermal coupling to the temperature, careful s-process calculations have been performed in Ref. [1] taking into account the neutron and temperature profiles in detail. The convective region was devided into 30 meshes, and the production and decay of ^{176}Lu was calculated in each mesh. After each time step of less than 1 h, the abundances from all zones were averaged to take into account convective mixing. Such time steps are sufficiently short compared to typical reaction rates of the thermal coupling between high-K and low-K states in ^{176}Lu (see Fig. 4).

It was found in Ref. [1] that the production ratio between ^{176}Lu and ^{176}Hf changes dramatically during the evolution of a helium shell flash (see Fig. 8 of Ref. [1]): At the onset of the flash a large ratio between ^{176}Hf and ^{176}Lu is found because of the dominating production of the ^{176}Lu isomer in the ^{175}Lu$(n, \gamma)^{176}$Lu reaction that decays to ^{176}Hf. As the temperature during the flash increases, ^{176}Hf is destroyed by neutron capture but only weakly reproduced by the decay of the ^{176}Lu isomer because of the thermal coupling of the low-K isomer to the long-living high-K ground state and the bypass of ^{176}Hf in the subsequent ^{176}Lu$(n, \gamma)^{177}$Lu neutron capture reaction. At the end of the flash neutron density and temperature drop down, and the initial ratio of ^{176}Hf and ^{176}Lu is almost restored. This means that the final abundances of ^{176}Hf and ^{176}Lu depend not only sensitively on temperature but also on the thermal conditions at the end of the helium shell flashes. This makes predictions of the ^{176}Hf and ^{176}Lu abundances extremely difficult and invalidates the simple interpretation of ^{176}Lu as *s*-process thermometer.

An ideal stellar *s*-process model should be able to reproduce the so-called overproduction factors $[N_s(176)/N_s(^{150}\mathrm{Sm})]/[N_\odot(176)/N_\odot(^{150}\mathrm{Sm})]$ (normalized to the *s*-only nucleus ^{150}Sm) of ^{176}Lu and ^{176}Hf simultaneously. The slow decay of the long-lived ^{176}Lu ground state in the interstellar medium prior to the formation of the solar system slightly reduces the abundance of ^{176}Lu and leaves the more abundant ^{176}Hf almost unchanged. Thus, overproduction factors of about $1.05 \pm 10\%$ for ^{176}Lu and $1.00 \pm 5\%$ for ^{176}Hf are the acceptable ranges [1]. Such a solution, the so-called "best case" with overproduction factors of 1.04 for ^{176}Lu and 0.95 for ^{176}Hf, has been found in Ref. [1] with the parameters $b^* = 0.022$ and $\tau = 80$ ps for the IS at 839 keV that correspond to an integrated cross section $I_\sigma^* = 71$ meV fm^2. Already a slightly increased integrated cross section (e.g., $b^* = 0.022$, $\tau = 50$ ps, $I_\sigma^* = 114$ meV fm^2) shifts the overproduction factors to their limits (1.08 for ^{176}Lu and 0.90 for ^{176}Hf) (see Table 7 of Ref. [1]).

The result of the present study shows that the integrated cross section of the IS at 839 keV is roughly one order of magnitude larger than the "best case" of Ref. [1] (see Sec. IV and Fig. 4). Therefore, the calculations in Ref. [1] were repeated with the larger integrated cross section derived in this work, i.e., with a significantly stronger coupling between the low-*K* isomer and the high-*K* ground state in ^{176}Lu.

Most of the ^{176}Lu is produced in the low-*K* isomer under *s*-process conditions that decays to ^{176}Hf. The stronger coupling transforms ^{176}Lu from the low-*K* isomer to the high-*K* ground state, thus increasing the overproduction factor of ^{176}Lu and reducing the overproduction factor of ^{176}Hf. With the stellar model used in Ref. [1] it was not possible to find a consistent solution within the given experimental errors of the neutron capture cross sections of the lutetium and hafnium isotopes and the uncertainty of the thermal coupling. For example, using the measured isomeric production ratio of 0.86 and an integrated cross section $I_\sigma^* = 850$ meV fm^2 from Sec. IV, the overproduction factors are 1.80 for ^{176}Lu and 0.61 for ^{176}Hf that is far out of the given range of $1.05 \pm 10\%$ for ^{176}Lu and $1.00 \pm 5\%$ for ^{176}Hf (see above).

A further test with a variation of the neutron production rate of the $^{22}\mathrm{Ne}(\alpha, n)^{25}\mathrm{Mg}$ reaction within a factor of two was also not successful. (For a detailed study of the influence of the neutron production rate in the $^{22}\mathrm{Ne}(\alpha, n)^{25}\mathrm{Mg}$ reaction on the *s*-process nucleosynthesis see Ref. [40].)

The astrophysical ingredients of the stellar *s*-process model have to be known with very high precision. Because of the extreme temperature dependence of the stellar transition rate λ^* between high-*K* and low-*K* states in ^{176}Lu, a possible solution of the problem may originate from modifications of the temperature profile or convective mixing during the helium shell flashes. It has to be noted that an increase of the integrated cross section I_σ^* by one order of magnitude (as determined in this work compared to the "best case" of Ref. [1]) may be compensated by a minor decrease in temperature by only about 1.5 keV leading to the same transition rate λ^* via the IS at 839 keV. Such minor modifications of the temperature profile will have only a small influence on other *s*-process branchings because most branchings are mainly sensitive to the neutron density. Although the temperature, which is "read" from the *s*-process thermometer ^{176}Lu, is only about 1.5 keV lower than in the temperature profile of the latest *s*-process study of the $A = 176$ branching [1], this interpretation of ^{176}Lu as *s*-process thermometer would by far be too simplistic because of the extremely sensitive interplay of nuclear and stellar physics in the final phase of helium shell flashes in AGB stars.

VII. CONCLUSIONS

It has been shown that the IS at 839 keV in ^{176}Lu leads to a much stronger coupling between low-*K* and high-*K* states in ^{176}Lu than assumed in a recent study [1]. This result is firmly based on a variety of experimental data for the IS at 839 keV. A further enhancement of the coupling may come from *K* mixing of two almost degenerate states at 725 keV; the analysis of the *K* mixing has to rely on theoretical arguments until now [2]. Further candidates for IS at higher and lower energies do not contribute significantly to the transition rate λ^* from high-*K* to low-*K* states in ^{176}Lu at *s*-process temperatures.

From the above results it is obvious that the *s*-process branching at $A = 176$ cannot be well described using the latest *s*-process model [1]. The nuclear physics ingredients of the model seem to be reliable and based on experimental data (except the *K* mixing of the two 7^- states at 725 keV). The neutron capture cross sections in this mass region have been measured carefully in the past few years, including the isomer branch in the $^{175}\mathrm{Lu}(n, \gamma)^{176}\mathrm{Lu}$ reaction [1,4]. The coupling of high-*K* and low-*K* states via IS is known from the combined analysis of all available experimental data. However, there is still an unsatisfactorily large range of allowed values for the integrated cross section I_σ^* under stellar conditions that should be reduced by further experiments (e.g., photoactivation using quasimonochromatic γ rays or using a quasistellar photon spectrum [41]; unfortunately, the relevant energy range is not easily accessible at the HIγS facility [42]). Such experiments may also address the influence of the suggested *K* mixing [2] on the transition rate.

After the nuclear physics input has been considerably improved for the IS at 839 keV, it was found that the astrophysical interpretation of the ^{176}Lu/^{176}Hf pair as an *s*-process thermometer is again in question due to strong overproduction of ^{176}Lu. The ultimate solution of this problem requires improved data for the *K* mixing of the two almost degenerate states at 725 keV, and it will further depend on refinements of the stellar physics in the final phase of helium shell flashes in AGB stars, thus providing deeper insight into the interesting physics of helium shell flashes.

ACKNOWLEDGMENTS

Encouraging discussions with A. Champagne and L. Lakosi are gratefully acknowledged.

[1] M. Heil, N. Winckler, S. Dababneh, F. Käppeler, K. Wisshak, S. Bisterzo, R. Gallino, A. M. Davis, and T. Rauscher, Astrophys. J. **673**, 434 (2008).
[2] V. Gintautas, A. E. Champagne, F. G. Kondev, and R. Longland, arXiv:0804.0223v1.
[3] P. Mohr, in proceedings of 10th Symposium on Nuclei in the Cosmos, PoS (NIC X) 081 (2008).
[4] K. Wisshak, F. Voss, F. Käppeler, and L. Kazakov, Phys. Rev. C **73**, 015807 (2006).
[5] O. Straniero, R. Gallino, and S. Cristallo, Nucl. Phys. **A777**, 311 (2006).
[6] S. Walter, F. Stedile, J. J. Carroll, C. Fransen, G. Friessner, N. Hollmann, H. von Garrel, J. Jolie, O. Karg, F. Käppeler, U. Kneissl, C. Kohstall, P. von Neumann-Cosel, A. Linnemann, D. Mücher, N. Pietralla, H. H. Pitz, G. Rusev, M. Scheck, C. Scholl, R. Schwengner, V. Werner, and K. Wisshak, Phys. Rev. C **75**, 034301 (2007).
[7] U. Kneissl, Bulg. Nucl. Sci. Trans. **10**, 55 (2005).
[8] J. J. Carroll, J. A. Anderson, J. W. Glesener, C. D. Eberhard, and C. B. Collins, Astrophys. J. **344**, 454 (1989).
[9] J. J. Carroll, M. J. Byrd, D. G. Richmond, T. W. Sinor, K. N. Taylor, W. L. Hodge, Y. Paiss, C. D. Eberhard, J. A. Anderson, C. B. Collins, E. C. Scarbrough, P. P. Antich, F. J. Agee, D. Davis, G. A. Huttlin, K. G. Kerris, M. S. Litz, and D. A. Whittaker, Phys. Rev. C **43**, 1238 (1991).
[10] L. Lakosi, I. Pavlicsek, and Á. Veres, Acta Phys. Hung. **69**, 169 (1991).
[11] L. Lakosi, N. X. Khanh, N. C. Tam, J. Sáfár, and I. Pavlicsek, Appl. Radiat. Isot. **46**, 435 (1995).
[12] P. Mohr, S. Brieger, G. Witucki, and M. Maetz, Nucl. Instrum. Methods Phys. Res. A **580**, 1201 (2007).
[13] J. Vanhorenbeeck, J. M. Lagrange, M. Pautrat, J. S. Dionisio, and Ch. Vieu, Phys. Rev. C **62**, 015801 (2000).
[14] Y. Watanabe, T. Mukoyama, and R. Katano, Phys. Rev. C **23**, 695 (1981).
[15] Á. Veres and I. Pavlicsek, Acta Phys. Hung. **28**, 419 (1970).
[16] E. B. Norman, T. Bertram, S. E. Kellogg, S. Gil, and P. Wong, Astrophys. J. **291**, 834 (1985).
[17] L. Lakosi, N. X. Khanh, N. C. Tam, J. Sáfár, I. Pavlicsek, and A. Petõ, Appl. Radiat. Isot. **46**, 433 (1995).
[18] C. Doll, H. G. Börner, S. Jaag, F. Käppeler, and W. Andrejtscheff, Phys. Rev. C **59**, 492 (1999).
[19] N. Klay, F. Käppeler, H. Beer, G. Schatz, H. Börner, F. Hoyler, S. J. Robinson, K. Schreckenbach, B. Krusche, U. Mayerhofer, G. Hlawatsch, H. Lindner, T. von Egidy, W. Andrejtscheff, and P. Petkov, Phys. Rev. C **44**, 2801 (1991).
[20] N. Klay, F. Käppeler, H. Beer, and G. Schatz, Phys. Rev. C **44**, 2839 (1991).
[21] P. Petkov, W. Andrejtscheff, and S. Avramov, Nucl. Instrum. Methods Phys. Res. A **321**, 259 (1992).
[22] K. T. Lesko, E. B. Norman, R.-M. Larimer, B. Sur, and C. B. Beausang, Phys. Rev. C **44**, 2850 (1991).
[23] R. A. Dewberry, R. K. Sheline, R. G. Lanier, L. G. Mann, and G. L. Struble, Phys. Rev. C **24**, 1628 (1981).
[24] K. E. G. Loebner, Phys. Lett. **B26**, 369 (1968).
[25] R. A. Ward and W. A. Fowler, Astrophys. J. **238**, 266 (1980).
[26] R. Gallino, C. Arlandini, M. Busso, M. Lugaro, C. Travaglio, O. Straniero, A. Chieffi, and M. Limongi, Astrophys. J. **497**, 388 (1998).
[27] Online database ENSDF, http://www.nndc.bnl.gov/ensdf/.
[28] M. S. Basunia, Nucl. Data Sheets **107**, 796 (2006).
[29] D. Belic, J. Besserer, C. Arlandini, J. de Boer, J. J. Carroll, J. Enders, T. Hartmann, F. Käppeler, H. Kaiser, U. Kneissl, M. Loewe, H. Maser, P. Mohr, P. von Neumann-Cosel, A. Nord, H. H. Pitz, A. Richter, M. Schumann, S. Volz, and A. Zilges, Nucl. Instrum. Methods Phys. Res. A **463**, 26 (2001).
[30] U. Kneissl *et al.* (to be published).
[31] D. Belic, C. Arlandini, J. Besserer, J. de Boer, J. J. Carroll, J. Enders, T. Hartmann, F. Käppeler, H. Kaiser, U. Kneissl, M. Loewe, H. J. Maier, H. Maser, P. Mohr, P. von Neumann-Cosel, A. Nord, H. H. Pitz, A. Richter, M. Schumann, S. Volz, and A. Zilges, Phys. Rev. Lett. **83**, 5242 (1999).
[32] D. Belic, C. Arlandini, J. Besserer, J. de Boer, J. J. Carroll, J. Enders, T. Hartmann, F. Käppeler, H. Kaiser, U. Kneissl, E. Kolbe, K. Langanke, M. Loewe, H. J. Maier, H. Maser, P. Mohr, P. von Neumann-Cosel, A. Nord, H. H. Pitz, A. Richter, M. Schumann, F.-K. Thielemann, S. Volz, and A. Zilges, Phys. Rev. C **65**, 035801 (2002).
[33] T. Kibédi, T. W. Burrows, M. B. Trzhaskovskaya, P. M. Davidson, and C. W. Nestor, Jr., Nucl. Instrum. Methods Phys. Res. A **589**, 202 (2008).
[34] B. Strömgren, Z. Astrophys. **4**, 118 (1932).
[35] P. Mohr, C. Angulo, P. Descouvemont, and H. Utsunomiya, Eur. Phys. J. A **27**, 75 (2006).
[36] P. Mohr, F. Käppeler, and R. Gallino, Phys. Rev. C **75**, 012802(R) (2007).
[37] A. Champagne (2008, private communication).
[38] M. Busso, R. Gallino, and G. J. Wasserburg, Annu. Rev. Astron. Astrophys. **37**, 239 (1999).
[39] O. Straniero, I. Domínguez, S. Cristallo, and R. Gallino, Publ. Astron. Soc. Pac. **20**, 389 (2003).
[40] C. Arlandini, F. Käppeler, K. Wisshak, R. Gallino, M. Lugaro, M. Busso, and O. Straniero, Astrophys. J. **525**, 886 (1999).
[41] P. Mohr, Zs. Fülöp, and H. Utsunomiya, Eur. Phys. J. A **32**, 357 (2007).
[42] A. Tonchev (2008, private communication).